Effect of the Convective Losses During Selective Laser Melting Process

Samia Aggoune, Farida Hamadi, El-Hachemi Amara,
Toufik Tamssaout, Karim Kheloufi and Kada Bougherara

Effect of the Convective Losses During Selective Laser Melting Process

Samia Aggoune[*1], Farida Hamadi[1], El-Hachemi Amara[1], Toufik Tamsaout[1], Karim Kheloufi[1], Kada Bougherara[1]

Abstract
This paper presents a numerical study aimed for understanding the effect of the convective losses during selective laser melting process. The initial powder distribution is obtained by discrete element method (DEM) calculation, while the temperature-velocity distributions are analyzed by ANSYS-FLUENT commercial code. Our study is developed in the mesoscale, and the main obtained results are for a laser power of 100 W and a scanning speed equal to 15 cm/s. It is shown that the convective losses is of important influence on the melting time of the powder as well as on the occurrence of the Marangoni convection. It was also noted that the values of the maximum temperature obtained when the pseudo stationary stage is reached are widely different in the two cases.

Keywords
Laser — Additive manufacturing — Melting — Selective laser melting — Stainless steel.

[1]Laser Material Processing Team, Centre for Development of Advanced Technologies, CDTA, PO. Box 17 Baba-Hassen, 163 Algiers, Algeria
[2]Department of Advanced Technological Processes and Projects, CDTA, PO. Box 17 Baba-Hassen, 16303 Algiers, Algeria
*Corresponding author: saggoune@cdta.dz

Introduction

In contrast to the traditional fabrication methods, using material removal, additive manufacturing is one of the modern processes allowing the building up of three-dimensional (3D) solid objects from the data of digital designed object based on CAD/CAM principles [1,2]. It can produce plastics, polymers, metals, ceramics and alternative to human tissue. The selective laser melting (SLM) process is one of the rapidly evolving additive manufacturing (AM) techniques, which falls under the category of powder bed fusion technique. This technology was first applied in the year 1997 [3]. It allows the re-use of the powder, which is one of its important advantage since it, leads to minimal waste of material. The SLM process has made an important impact in the sectors of manufacturing, automotive, aerospace, pharmaceutical, and electronics [4-8].

Numerical and experimental investigations are developed to understand the effects of the parameters used during the SLM process on the characteristics of the produced parts. We must emphasize that the conducted researches are extensive and cover different aspects such as laser scanning strategies, mechanical properties, and powder nature, among others. Kempen [9] combined different laser powers and scanning speeds to determine the optimal scanning strategy and hatch spacing, He scanned single line track for a given laser diameter and layer powder thickness. Wang *et al.* [10] have correlated the morphology of single line scan with the heat laser energy input numerically. From other side the numerical models allowed to investigate the impact of the process parameters on the characteristics of the material. Simulations advantages are the identification of the proper parameters without conducting expensive experimental testing. During the recent years, investigations have been conducted by implementing thermal, microstructural, mechanical models, and computational fluid dynamics (CFD) models [11, 12]. Finite element modeling (FEM) [13, 14] was used for understanding the fluid dynamics occurring during the process of laser-matter interaction. The complex thermo kinetics of the process is influenced by the process parameters and thermo physical properties of the material. Sun *et al.* [15] proposed optimizing parameters by using the Taguchi method and regression analysis, it was found that the most significant factors for the process could be classified as, powder thickness, scanning strategy, linear energy density, hatching distance.

In this paper, a mesoscale transient 3D model, for selective laser melting process (SLM) is studied. A model is developed to investigate the effect of

convection losses on one single pass of laser on the 316L stainless steel. The model implementation for the numerical calculation is based on ANSYS/FLUENT commercial software. Our approach solves the heat transfer equations by including the phase change, and the laser effect is modeled as a three dimensional Gaussian volumetric energy source that is imposed on a two-dimensional surface. By looking at the melting and solidification of the 316L stainless steel powder, we simulate and analyze the temperature and velocity profiles for fixed values of the processing parameters when the convection is included and when it is neglected.

Modeling

We consider fixed values of the processing such as a laser beam power P=100W and a laser beam radius r_l=75μm, for a powder layer thickness of 100μm and a scanning speed equal to 0.15 m/s. The system is in an air protective atmosphere gas. All the thermal properties and the process parameters are listed in **table 1.**

   1. **Hypotheses:** A number of simplifying assumptions are necessary to solve of the equations of our model:

 -The metallic liquid is newtonian, viscous, incompressible and laminar.
 - The Boussinesq approximation is neglected.
 - Radiation and vaporization are neglected.
 - Gaussian distribution of the laser spot with (TEM$_{00}$) mode is used.

The problem geometry, the meshing grid and the related boundary conditions were prepared by the means of the pre-processor GAMBIT, whereas the numerical solving of the the Navier-Stokes equations was performed the processor ANSYS/FLUENT. The so-called volume of fluid (VOF) model is well appropriate for tracking sharp interfaces. In our case, the interface is between two immiscible fluids, namely the molten stainless steel and the air. The states change of the stainless steel from liquid to solid or from solid to liquid during the melting or cooling is treated by 'Melting and Solidification' model. This model is implemented in ANSYS/FLUENT by an enthalpy based phase change approach; it includes a mushy region around the melting point, where the material is linearly changing from solid to liquid. To deal with our laser source of energy term and some temperature dependent physical properties (density and surface tension) user defined functions (UDFs) written in C++ must be included during the computing process.
Our model is divided into three zones: a melted zone, a solid zone, and air. As we can see from the figure 1, the grid is tightened near the interfaces, where the gradients of temperatures and velocities are important. Elsewhere, the grid spacing is larger. The assigned time step for this mesoscale simulation was 10^{-8} s and the convergence criterion on the residuals

of each equation was less than 10^{-4} except for the energy it is 10^{-6}. The thin layer of stainless steel powder (100 μm) is resting on a thick substrate (400 μm) of the same material, then, we can set the bottom of this later adiabatic in order to represent the very low thermal gradients at this distant boundary.
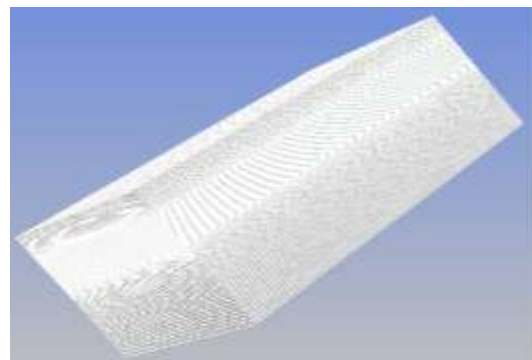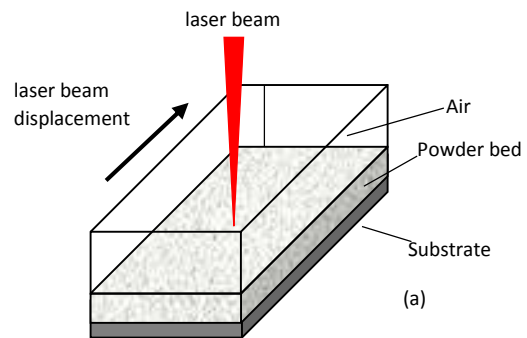

(a)

(b)

Figure 1. The computational domain (environing air, powder bed, substrate) (a), and its mesh (b)

Table 1. The thermal properties and the process parameters chosen in this simulation.

Parameter	Value
Liquidus temperature	1762 (K)
Solidus temperature	1700 (K)
Enthalpy change of melting	270000 (J/Kg)
Absorption coefficient	0.45
Density	7800 (Kg/m^3)
Viscosity	0.0033 (Pa.s)
Surface tension	1.6 (N/m)
Thermocapillary coefficient	-0.3e-3 (N/m.K)
Laser power	100 (W)
Scanning speed	0.15(m/s)
Spot radius	70 (μm)
Layer thickness	105 (μm)

   2. **Equations**

The continuity (1), momemtum (2) and energy (3, 4) equations are written as follows:

$$\frac{\partial u}{\partial x} + \frac{\partial v}{\partial y} + \frac{\partial w}{\partial z} = 0 \qquad (1)$$

$$\frac{\partial \vec{V}}{\partial t} + \vec{V} grad(\vec{V}) = -\frac{1}{\rho} grad(p) + \mu\Delta(\vec{V}) + \rho_0 \vec{g} - \gamma k\vec{n} + \frac{\partial \sigma}{\partial T}[\vec{V}T - \vec{n}(\vec{n}.\vec{V}T)] \qquad (2)$$

$$\rho\, C_p\, \frac{\partial T}{\partial t} = -\frac{\partial}{\partial x}\left(k\frac{\partial T}{\partial x}\right) - \frac{\partial}{\partial y}\left(k\frac{\partial T}{\partial y}\right) - \frac{\partial}{\partial z}\left(k\frac{\partial T}{\partial z}\right) + Q \quad (convection\ not\ included) \qquad (3)$$

$$\rho\, C_p\, \frac{\partial T}{\partial t} = -\frac{\partial}{\partial x}\left(k\frac{\partial T}{\partial x}\right) - \frac{\partial}{\partial y}\left(k\frac{\partial T}{\partial y}\right) - \frac{\partial}{\partial z}\left(k\frac{\partial T}{\partial z}\right) + Q - \frac{h(T-T_0)}{e} \quad (convection\ included) \qquad (4)$$

In the following, we focus on the evolution of the temperature and velocity profiles when convection is included and when it is neglected.

Results and Discussion

Using the We analyze in the following the convection losses impact for one laser pass during selective laser melting (SLM) process via the profiles of temperature and velocity profiles at different times and positions. At simulation starting, we note on figure 2 that the Gaussian laser distribution on the horizontal plane, shows the higher temperature is in the central region, while it is lower at the periphery. In addition, we can see that the fusion is observed at time t= 3.233 10^{-4}s in the case when the convective losses are not included. When these losses are included, the duration to get powder fused must exceed the double of the time such as t= 8.8 10^{-4}s.

Actually, taking into account the convective losses in the powder bed, the energy coming from the laser will no longer be localized in small region but it will be diffused

in a larger space, so the heat affected zone (HAZ) will be larger, as shown by the same figure.
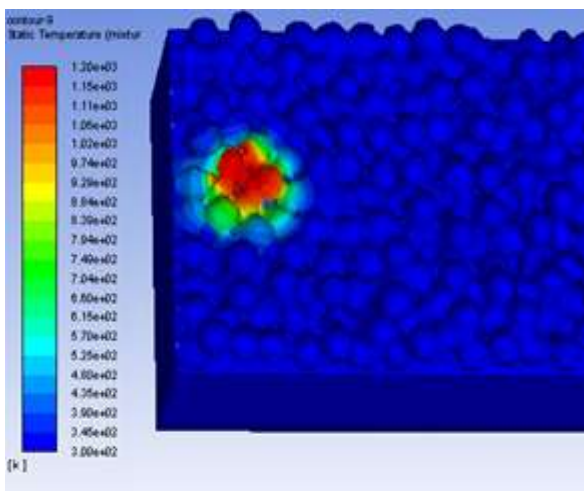
(a)
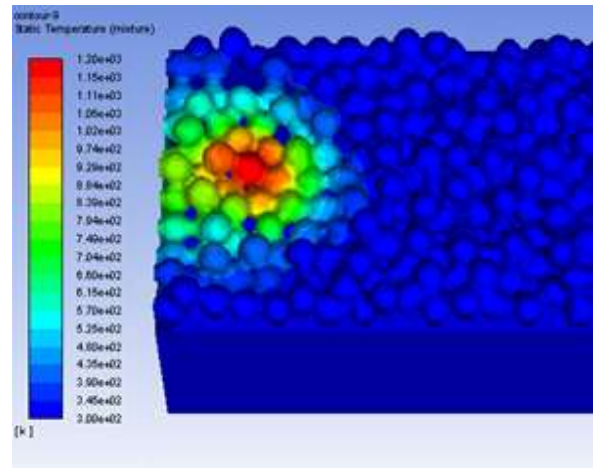
(b)

Figure 2. Temperature distributions at the beginning of fusion (a) losses by convection no included at t=3.23e-04s, (b) losses by convection included at t=8.82 e-04s

If we choose a time whatever of the pseudo stationary regime, for example, time t= 2.16 10^{-3} s, corresponding to the case where convection losses are not included, we can remark from figure 3 that the Marangoni convection is appeared. Therefore, the graph of velocity versus the displacement direction shows then two peaks (maximums) of velocity.

The first peak is observed at position y=-0.37 mm with a value of V_{max1} = 1.15m / s and the second peak at position y=-0.32 mm with a smaller value equals to V_{max2} = 0.78m / s.
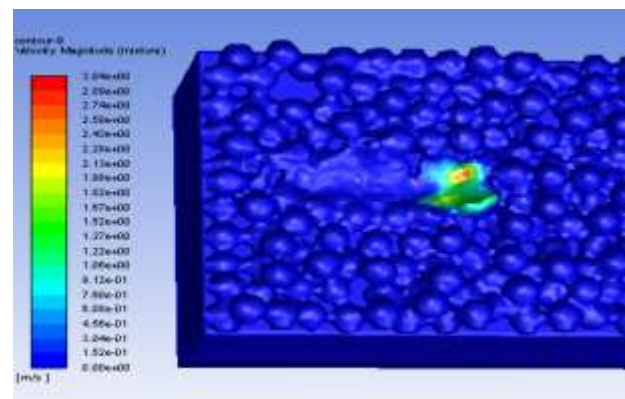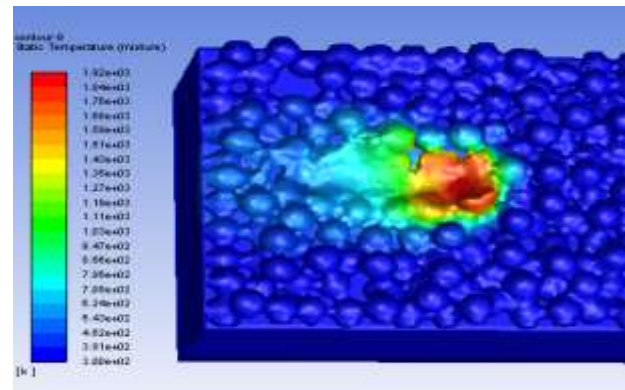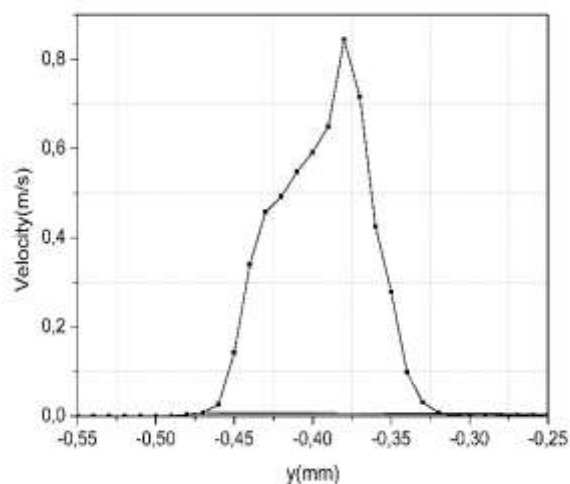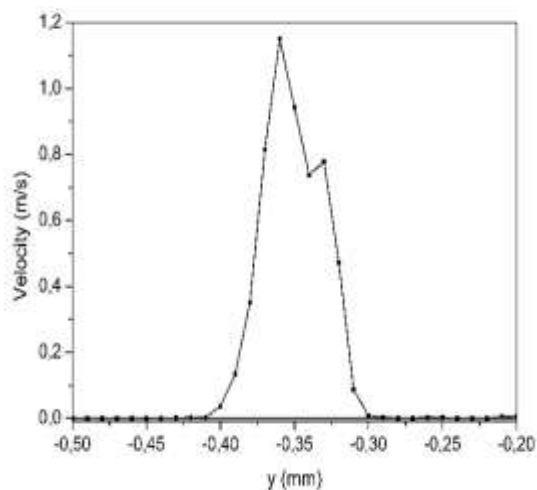
Figure 3. Temperature and velocity profiles at 2.16 e-3s when losses convection are not included

We note on figure 4 that the Marangoni convection disappears at the same time (t = 2.16 e-03s) in the case where convective losses are taken into account. Therefore, we have only one peak of velocity, observed at y = -0.383 mm with a value of V_{max} = 0.86 m/s.

Figure 4. Temperature and velocity profiles at 2.16 e-3s when losses convection are included.

In the figures below, we can also note that the maximum temperature reached at the stable stage in the two cases are highly different. If the convective losses are not taken into account, the maximum temperature reached is 1850K, and for the case where these losses are taken into account, this maximum is much lower and it is 1200K, see figures (5, 6) below.

To validate the accuracy of our simulation results, we have compared some of them with those of Khairallah et al. [16, 17]. We can conclude that the differences are provided from the omission of the radiation and natural convection (buoyancy) in our case.
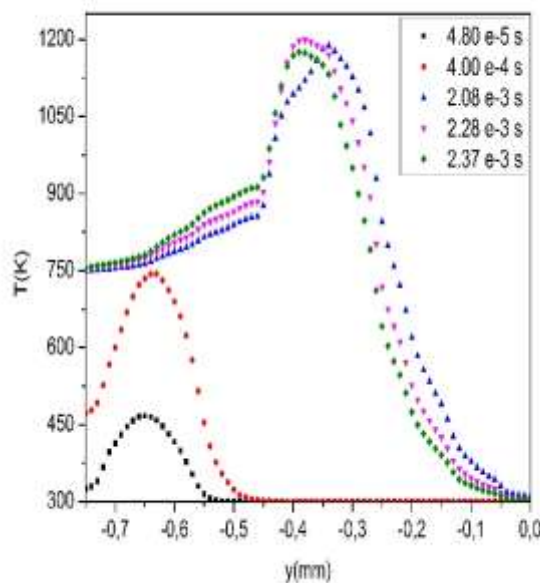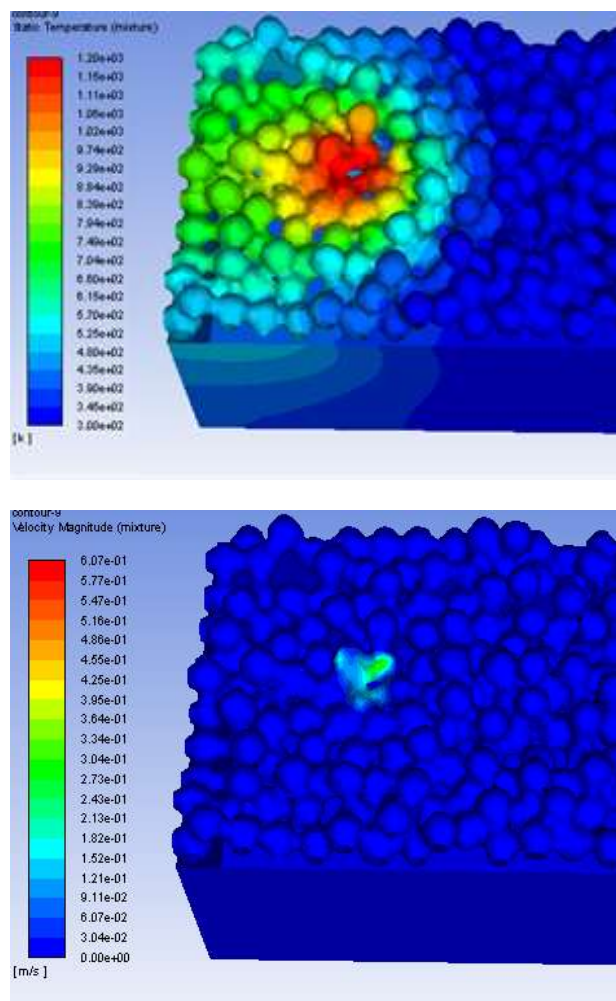

Figure 5. Maximum temperature (1205 K) at the stable stage when convection losses are included
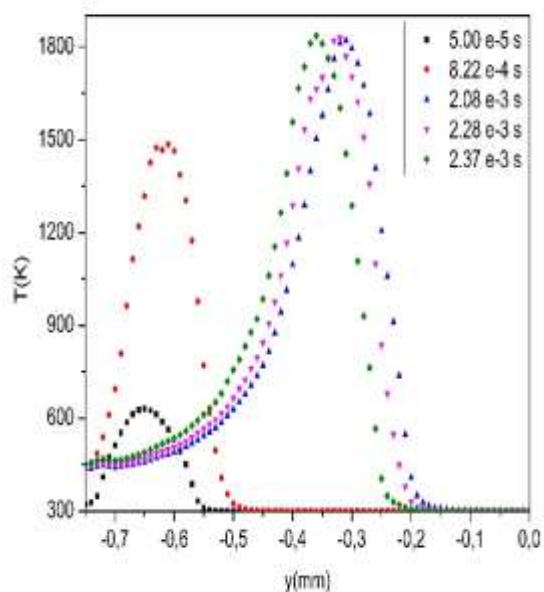
Figure 6. Maximum temperature (1850 K) at the stable stage when convection losses are not included

Conclusion

From the implementation of our model for the study of the effect of convection losses on the phenomena observed during selective laser melting (SLM) on powder beds, we can conclude that for our operating parameters, the convection losses plays a significant role in the heat transfer rate during this process.

References

[1] I. Gibson, D.W. Rosen, B. Stucker, Additive manufacturing technologies, Springer. 2010.

[2] DebRoy, T.; Wei, H.L.; Zuback, J.S.; Mukherjee, T.; Elmer, J.W.; Milewski, J.O.; Beese, A.M.; Wilson-Heid, A.;De, A.; Zhang, W. Additive manufacturing of metallic components—Process, structure and properties.Prog. Mater. Sci., 92, 112–224, 2018.

[3] Colin, C.; Bartout, J.D.; Shaker, E.; Marchat, D.; Nimal, D. Selective Laser Melting Process. Patent No.EP2978727, 3 February, 2016.

[4] Olakanmi, E.O.; Cochrane, R.F.; Dalgarno, K.W. A review on selective laser sintering/melting (SLS/SLM)of aluminium alloy powders: Processing, microstructure, and properties. Prog. Mater Sci. 74, 401–477, 2015

[5] Aramian, A.; Sadeghian, Z.; Razavi, S.M.J.; Prashanth, K.G.; Berto, F. E_ect of selective laser meltingprocess parameters on microstructural and mechanical properties of TiC-NiCr cermet. Cer. Int., in press, 2020.

[6] Tang, H.P.; Qian, M.; Liu, N.; Zhang, X.Z.; Yang, G.Y.; Wang, J. E_ect of powder reuse times on additivemanufacturing of Ti-6Al-4V by selective electron beam melting. JOM, 67, 555–563,, 2015.

[7] Salman, O.O.; Gammer, C.; Eckert, J.; Salih, M.Z.; Abdulsalman, E.H.; Prashanth, K.G.; Scudino, S. Selectivelaser melting of 316L stainless steel: Influence of TiB2 addition on microstructure and mechanical properties.Mater. Today Commun. 21, 100615, 2019.

[8] Suryawanshi, J.; Prashanth, K.G.; Ramamurty, U. Mechanical behavior of selective laser melted 316L stainlesssteel. Mater. Sci. Eng. A, 696, 113–121, 2017.

[9] K. Kempen, Expanding the Materials Palette for Selective Laser Melting of Metals, KU Leuven, Belgium, 2015.

[10] L. Wang, Q. Wei, Y. Shi, J. Liu, W. He, Experimental investigation into the singletrack of Selective Laser Melting of IN625, Adv. Mater. Res. 233-235, 2844–2848. 2011.

[11] K. Antony, N. Arivazhagan, K. Senthilkumaran, "Numerical and experimental investigations on laser melting of stainless steel 316L metal powders", J. Manuf. Process. **16 (3)**, 345–355, 2014.

[12] S. Mohanty, J. Hattel, "Cellular scanning strategy for selective laser melting: Capturing thermal trends with a low-fidelity, pseudo-analytical model", Math. Probl. Eng., ID 715058, 2014.

[13] L.E. Criales, Y.M. Arısoy, T. Özel, "Sensitivity analysis of material and process parameters in finite element modeling of selective laser melting of Inconel 625", Int. J. Adv. Manuf. Technol. **86 (9–12)**, 2653–2666, 2016.

[14] Y. Huang, L.J. Yang, X.Z. Du, Y.P. Yang, "Finite element analysis of thermal behavior of metal powder during selective laser melting", Int. J. Therm. Sci. **104**, 146–157 2016.

[15] J. Sun, Y. Yang, D. Wang, Parametric optimization of selective laser melting for forming Ti6Al4V samples by Taguchi method, Opt. Laser Technol. 49,118–124, 2013.

[16] S.A. Khairallah, A.T. Anderson, A. Rubenchik, and W.E. King: Acta Mater., 2016, vol. 108, pp. 36–45.

[17] S. Ly, A.M. Rubenchik, S.A. Khairallah, G. Guss, and M.J. Matthews: Sci. Rep., 2017, vol. 7, p. 4085.